Plant, Cell and Environment (2009) **32**, 250–258 doi: 10.1111/j.1365-3040.2008.01917.x

An energy balance from absorbed photons to new biomass for *Chlamydomonas reinhardtii* and *Chlamydomonas acidophila* under neutral and extremely acidic growth conditions

UWE LANGNER, TORSTEN JAKOB, KATJA STEHFEST & CHRISTIAN WILHELM

University of Leipzig, Institute of Biology I, Department of Plant Physiology, Johannisallee 23, D-04103 Leipzig, Germany

ABSTRACT

***Chlamydomonas* is one of the most well-studied photosynthetic organisms that had important biotechnological potential for future bioproductions of biofuels. However, an energy balance from incident photons to the energy stored in the new biomass is still lacking. In this study, we applied a recently developed system to measure the energy balance for steady state growth of *Chlamydomonas reinhardtii* grown at pH 6.5, and *C. acidophila* that was grown at pH 6.5 and 2.6. Energy use efficiency was quantified on the basis of light absorption, photosynthetic quantum yield, photosynthetic and respiratory quotient, and electron partitioning into proteins, carbohydrates and lipids. The results showed that lower growth rates of *C. acidophila* under both pH conditions were not caused by the differences in the photosynthetic quantum yield or in alternative electron cycling, but rather by differences in the efficiency of light absorption and increased dark respiration. Analysis of the macromolecular composition of the cells during the light phase showed that *C. acidophila* uses biosynthetic electrons preferentially for carbohydrate synthesis but not for synthesis of lipids. This led to a strong diurnal cycle of the C/N ratio and could explain the higher dark respiration of *C. acidophila* compared with *C. reinhardtii*.**

Key-words: *Chlamydomonas*; acidic condition; biomass; C/N ratio; energy use efficiency; growth; macromolecules.

INTRODUCTION

Chlamydomonas strains are widely used as model organisms for photosynthesis (Finazzi & Forti 2004; Rochaix 2004), basic cell research including rhythms (Mittag & Wagner 2003), signal transduction (Schmidt, Geßner & Luff 2006) and for algal biomass cultures (Mussgnug *et al.* 2007). Because the genome is fully sequenced and an efficient transformation system is available (Purton 2007), this genus is intended to become a future hydrogen producer (Grossman & Rokhsar 2007; Melis, Seibert & Ghirardi 2007). *Chlamydomonas* is one of the best candidates to be used in system biology because data platforms exist at the levels of the genome, transcriptome, proteome and metabolome (Davies & Grossman 1998; Dent, Han & Niyogi 2001; Stauber & Hippler 2004). The aim is to understand cell function in a way that all input parameters can be linked in a network that can predict the relevant output parameters. In the case of a photosynthetic organism, it is of special interest to understand the regulation of all steps involved from light to growth.

In the last decade, fluorescence techniques have tremendously advanced the study of primary production in the laboratory and in nature to quantify primary production, in addition to the traditional techniques including gas exchange measurements and radio carbon uptake (for a review see Falkowski & Raven 1997). The *in situ* fluorescence techniques were an important advance because the absorption cross-section and photosystem II (PSII) quantum yield can be measured simultaneously (Suggett *et al.* 2003). Many studies have shown that *in situ* electron transport rates can show a linear relationship to oxygen production or to carbon uptake. From these studies, it has been concluded that fluorescence-based electron transport measurements match gas exchange data and yield real values of primary production (Suggett, Maberly & Geider 2006). Because fluorescence techniques are relatively inexpensive and easy to handle, it seemed an appropriate instrumentation to control the efficiency of algal mass cultures, because any change in photosynthetic efficiency can be monitored online (for a review see Prasil *et al.* 2008).

However, the quantitative relationships among electron transport rates, carbon assimilation and the new biomass are still not completely understood. The first major question is the amount of so-called 'alternative electrons'. The term is used to mean electrons transported by PSII that are not used for carbon assimilation, but for cyclic electron flow, or to reduce oxygen again to start the water–water cycle (Asada 2000), or that have been lost by photorespiration. It has been assumed, but not convincingly illustrated, that this alternative electron transport increases under stress conditions (Geel, Versluis & Snel 1997). The second question concerns all events during the dark phase, for example,

Correspondence: C. Wilhelm. Fax: +49 341 9736899; e-mail: cwilhelm@rz.uni-leipzig.de

respiration, nitrate reduction, etc. The third question is centred on an incomplete understanding regarding the fate of the photosynthates in the metabolism to produce new cells. The photosynthetic equation stoichiometrically equates the rates of oxygen evolution and carbon dioxide fixation under the condition that carbohydrates are synthesized. However, the overall macromolecular composition of a single eukaryotic cell contains a variable proportion of proteins to carbohydrates to lipids. Because proteins and lipids are more greatly reduced than carbohydrates, we could expect that the demand of electrons to incorporate one carbon atom into the biomass is much higher than four.

This problem has recently been addressed by Wagner, Jakob & Wilhelm (2006) by running an energy balance from the incident photons to the new biomass where its reduction degree was measured by determining the ratio carbohydrates to proteins to lipids using Fourier transform infrared (FTIR) spectroscopy (Jakob *et al.* 2007). They showed that the ratio of electrons transported by PSII and new biomass is highly variable, and depends not only on the light climate, but also on nutrient availability. In the first study by Wagner *et al.* (2006), it became obvious that the efficiency of biomass formation is not uniform between a green alga and a diatom, and in particular, the ratio of alternative electron cycling was found to be significantly higher in the chlorophyte than in the diatom under fluctuating light conditions.

In this study, we applied this approach to compare two *Chlamydomonas* strains grown under neutral and extreme acidic conditions. The aim of this study was to run an energy balance for *Chlamydomonas* under balanced growth conditions and to examine how the alternative electron cycling, dark respiration and the changes in the macromolecular composition influence the energy balance from the photons into the biomass under extreme acidity. We tested whether energy balancing is a suitable approach to explain the fact that *C. acidophila* shows substantially lower growth rates than *Chlamydomonas reinhardtii*, but the metabolic costs for proton compensation are too low to explain this difference (Messerli *et al.* 2005).

MATERIALS AND METHODS

Culture conditions

Experiments were performed with the chlorophyte *C. reinhardtii* (SAG 11-32b, Sammlung für Algenkulturen, Göttingen, Germany) in a semi-continuous culturing system (Wilhelm & Wild 1984). Illumination was provided with a day length of 13 h by an Osram L36W/25-1 Universal-white (Osram, München, Germany) providing a light intensity of 180 μmol photons m^{-2} s^{-1}. Cells were grown in modified Woods Hole medium according to Nichols (1973). The cell cultures were diluted with fresh medium, always at the same time point at the beginning of the light period. To keep the self-shading of algal cells to a minimum, the Chl *a* content was adjusted to either 1.5 mg L^{-1} for *C. reinhardtii* and *C. acidophila* pH 6.5 or, because of the lower ratio, Chl *a* $cell^{-1}$ to 2 mg L^{-1} in *C. acidophila* pH 2.6. Under each growth condition, measurements for the determination of photosynthesis rates and biomass production (see further discussion) began after the cell culture reached a constant growth rate for at least 5 d.

During the light phase, a sample (10 mL) was taken out of the culture vessel every 2 h. Three milliliters of this sample were placed in the cuvette of the oxygen/fluorescence measuring device (photosynthetic light dispenser, Topgallant, Salt Lake City, UT, USA) to measure fluorescence- and oxygen-based photosynthesis rates (see following discussion). From the same sample, the measurements of cell number, chlorophyll content, *in vivo* absorption and FTIR measurement were performed.

Measurement of growth, photosynthesis rates and carbon-related biomass production

Growth rates (μ) were calculated as follows:

$$\mu = D + \left(\frac{dx}{dt \cdot x_0} \right), \quad (1)$$

with

$$D = \frac{f}{V}, \quad (2)$$

where D is the dilution rate, f is dilution volume, V is the volume of the culture vessel, dx is the change in cell number during time interval dt and x_0 is the cell number before time interval dt. Cell numbers were measured using a cell counter (Z2 Coulter Counter; Coulter Electronics Inc., Miami, FL, USA). In parallel, the bio-volume of cells was detected based on impedance measurement of electric conductivity of liquid (Isoton II Diluent, Beckman Coulter; Krefeld, Germany). Dilution volume and cell numbers were always determined at the beginning of the light period.

Measurement of fluorescence- and oxygen-based photosynthesis rates (P_F and P_O, respectively), the calculation of photosynthetically absorbed radiation (Q_{phar}), and the theoretical biomass production were performed as described in Wagner *et al.* (2006). Essentially, it is assumed that the fluorescence-based photosynthesis rate (P_F) is the maximum amount of electrons (expressed as oxygen evolution) transported through the electron transport chain. P_F (pmol O_2 $cell^{-1}$ d^{-1}) can be calculated as

$$P_F = \Phi_{PSII} \times Q_{phar} \times 0.5 \times 0.25, \quad (3)$$

where Φ_{PSII} is the effective fluorescence quantum yield of PSII (Genty, Briantais & Baker 1989) at a photon fluence rate of 180 μmol quanta m^{-2} s^{-1}, and Q_{phar} (pmol quanta $cell^{-1}$ d^{-1}) is the daily amount of cellular absorbed radiation. The factors 0.5 and 0.25 are based on the assumption that the linear transport of one electron requires two quanta, and that four electrons are required for the evolution of one

molecule oxygen. A pulse amplitude-modulated fluorometer (PAM 101, Walz, Effeltrich, Germany) was used for the determination of Φ_{PSII}.

With the knowledge of the emission spectra of the light source and the Chl *a*-specific absorption, it is possible to estimate the amount of the photosynthetically absorbed radiation (Q_{phar}) by the algal culture based on the following equation (according to Gilbert *et al.* 2000):

$$Q_{phar} = \int_{400nm}^{700nm} Q(\lambda) - Q(\lambda) \cdot e^{[-a^*_{phy}(\lambda)(\mathrm{Chl}\,a)d]} d\lambda \quad (4)$$

where Q_{phar} is the photosynthetically absorbed radiation (μmol photons m^{-2} s^{-1}), Q is the photosynthetically available (incident) radiation (μmol photons m^{-2} s^{-1}) in dependence of the light source, a^*_{phy} is the Chl *a*-specific *in vivo* absorption coefficient [m^2 (mg Chl *a*)$^{-1}$], and d is the optical path length (m). The concentrations of Chl *a* and Chl *b* were determined spectrophotometrically in 80% acetone using the equations of Ziegler & Egle (1965).

Part of the absorbed radiation is dissipated non-photochemically as fluorescence and heat. These losses were estimated as a relative proportion of Q_{phar} using

$$\sum_{NPQ+F} = (1 - \Phi_{PSII}). \quad (5)$$

Oxygen-based photosynthesis rates (P_O, pmol O_2 $cell^{-1}$ d^{-1}) and mitochondrial respiration rates (R, pmol O_2 $cell^{-1}$ d^{-1}) were measured using a Clark-type electrode (MI 730, Microelectrodes Inc., Bedford, NH, USA). For this purpose, cells were taken directly from the culture vessels every 2 h and were placed in the measurement chamber of the oxygen electrode. To determine net photosynthesis rates, cells were illuminated for 5 min with the same amount of incident light as applied in the culturing system. The mitochondrial dark respiration was measured subsequent to the illumination period. Thus, respiration rates should represent the mitochondrial oxygen consumption during the light period. Consequently, this light-affected respiration is denoted as R_L. Respiratory losses during the scotophase (denoted as R_D) were approximated by measurements of oxygen gas exchange of samples taken from the culture vessel at the end of the dark period. Photosynthetic gross oxygen production was derived by correcting net oxygen evolution rates for the corresponding dark respiration. It is assumed that the oxygen-based photosynthesis rate represents the electron transport rate at PSII, which is biased by light-dependent, alternative electron pathways, like the oxygen-consuming Mehler reaction or the electron cycle around PSII. Thus, the equation

$$P_{alt} = (P_F \times P_O) \times 4 \quad (6)$$

describes the amount (pmol electrons $cell^{-1}$ d^{-1}) of electrons consumed in processes other than CO_2 fixation by Calvin cycle. The factor 4 takes into account that four electrons per molecule oxygen are released at PSII. P_{alt} can be expressed as the ratio of absorbed photons by

$$P_{alt}^{\%Q_{phar}} = \frac{P_{alt} \times 2}{Q_{phar}} \quad (7)$$

that assumes that the linear electron transport requires two photons per electron released at PSII.

The carbon-related biomass production (B_C, pg C $cell^{-1}$ d^{-1}) was derived from the following equation:

$$B_C = C_{cell} \times \mu, \quad (8)$$

where C_{cell} is the cellular carbon content (pg C $cell^{-1}$) obtained from the measurement of the elemental composition (see following discussion) and μ is the daily growth rate.

From the net photosynthesis rate P_{Onet} a theoretical carbon production rate per unit time (B_O, pg C $cell^{-1}$ dt^{-1}) can be approximated:

$$B_O = [(P_{Onet}/PQ) - (R \times RQ)] \times 12, \quad (9)$$

where PQ and RQ are the photosynthetic and respiratory quotient, respectively, and 12 is the conversion factor from pmol to pg carbon.

Photosynthetic and respiratory quotient

All measurements of gas exchange to calculate the photosynthetic and the respiratory quotients were performed using a respirometer (Biometric Systems, Weiterstadt, Germany) as described in Wagner *et al.* (2006). The photosynthetic (PQ) and the respiratory quotient (RQ) were calculated with the following equations:

$$PQ = [OER]/[CER] \quad (10)$$

$$RQ = [CER]/[OER], \quad (11)$$

where $[OER]$ is the absolute O_2-exchange rate (μL h^{-1}) and $[CER]$ is the absolute CO_2-exchange rate (μL h^{-1}).

Elemental and biomass composition

The elemental composition was measured according to Wagner *et al.* (2006) using a CHNSO analyser (vario EL, Analytik Jena GmbH, Jena, Germany). The FTIR microspectroscopy method was used to follow the changes in the main biochemical cell compounds. The correlation of the quantitative determination of the biomass composition in microbial cells by FTIR spectroscopy and chemical analyses was demonstrated in Grube *et al.* (1999). In the present study, a modified version of the Stehfest, Toepel & Wilhelm (2005) method was used. During the light periods, samples were taken every 2 h from the culture vessel. From the washed and concentrated cell suspension, samples of 1 μL (with ~5×10^5 cells) were placed on a microtiter plate and dried at 40 °C for 5 min. Infrared (IR) spectra were recorded in the range of 4000–700 cm^{-1} without further

sample treatment in transmission mode with 32 scans oversampling to enhance the signal-to-noise ratio (Vector 22 laser unit, HTS-XT microtiter module, OPUS and OPUSLab v5.0 software, Bruker Optics, Karlsruhe, Germany). Spectral quota of carbohydrates, proteins, lipids and nucleic acids were quantified by recalculating baseline-corrected spectra with reference spectra of glucose, bovine serum albumin, palmitic acid triglyceride and RNA, respectively. Apart from nucleic acids (Invitrogen, Carlsbad, CA, USA), all substances were obtained from Sigma (St Louis, MO, USA). Spectra of reference substances were recorded at a concentration range of 0.5–30 μg under the conditions described earlier. For this purpose, substances were dissolved in distilled water (glucose, bovine serum albumin and nucleotides) or in trichloromethane (palmitic acid triglyceride). A calibration curve was determined for each substance, which allowed a correlation of spectral quota with the amount of the substance at a characteristic absorption frequency (glucose, 1150 cm^{-1}; bovine serum albumin, 1545 cm^{-1}; palmitic acid triglyceride, 2849 cm^{-1}; RNA 1243 cm^{-1}).

The biomass composition was calculated by analysing IR spectra in the frequency range of 3100–700 cm^{-1}. IR spectra of cells and reference substances were analysed using a linear combination algorithm. Spectral quota of carbohydrates, proteins, lipids and nucleic acids were yielded as factors and multiplied with the respective reference spectra resulting in defined absorption intensities. By applying absorption intensities of each reference spectrum at its characteristic frequency, the amounts of cellular substances were calculated from aligned calibration curves. Calculated data were then quoted as weight percent per dry weight. The method is validated by conventional biochemical procedures (Stehfest 2006).

The synthesis rates of carbohydrates, proteins and lipids per unit time (B_{FTIR}, pg $cell^{-1}$ dt^{-1}) can be expressed by

$$B_{FTIR} = [B_O/(C/DW)] \times c_{MC}, \quad (12)$$

where *C/DW* is the ratio carbon per dry weight and c_{MC} is the fraction of the respective macromolecular compounds per dry weight.

RESULTS

Growth rate and cellular growth efficiency

In the present study, the growth rate of *C. reinhardtii* at pH 6.5 was 1.5 and almost twofold higher than *C. acidophila* grown at pH 2.6 and pH 6.5, respectively (Table 1). Dividing the growth rate by the numbers of photons absorbed per cell and day during the light phase yields a ratio that indicates the cellular growth efficiency. Surprisingly, this ratio was highest in *C. acidophila* at pH 2.6, followed by *C. reinhardtii* and *C. acidophila* at pH 6.5 (Table 1).

The growth rate of a phytoplankton cell culture is determined by all cellular processes, from light absorption, via the rate and quantum efficiency of the photosynthetic electron supply and energy losses by respiratory processes to the amount of carbon incorporated into the biomass of a cell. The following data show how the different growth rates in the three investigated species can be explained through an energy balance that takes into account the cellular processes noted above.

Changes in bio-optical properties

The first step in an energy balance is to estimate the amount of absorbed energy. Figure 1a shows that in *C. reinhardtii* a higher cellular chlorophyll content was observed compared with *C. acidophila*. In particular, in *C. acidophila* grown at pH 2.6, the pigment content per cell was reduced to about 65% in comparison with *C. reinhardtii*. A look to the Chl *a*/*b* ratio (Table 1) demonstrates that *C. acidophila* synthesizes greatly reduced light harvesting complexes compared with *C. reinhardtii*. Because the antenna proteins bind not only chlorophyll, but also most of the carotenoids, their contribution to the total absorption is decreased. The change in absorption efficiency is made even more complex by significant size variation of the cells (Fig. 1b), which becomes obvious in the ratio Chl/BV (chlorophyll per biovolume; Fig. 1c). Here, the difference between *C. reinhardtii* and *C. acidophila* at pH 2.6 is minor, whereas the cells of *C. acidophila* at pH 6.5 are enlarged.

Both parameters – chlorophyll packaging on the one hand and cell size on the other – influence the absorption

Table 1. Cellular parameters and growth of *Chlamydomonas reinhardtii* at pH 6.5 and *C. acidophila* at pH 2.6 and 6.5

Parameter	*C. reinhardtii* pH 6.5	*C. acidophila* pH 2.6	*C. acidophila* pH 6.5
Chl *a*/*b*	2.7 ± 0.04	4.2 ± 0.2	4.8 ± 0.3
Q_{phar}[a]	74 ± 1	45 ± 4	61 ± 3
DW/cell[b]	43.3 ± 1.4	50.3 ± 3	52.1 ± 4.4
μ[c]	0.50 ± 0.03	0.34 ± 0.03	0.26 ± 0.04
Growth efficiency[d]	6.8 ± 0.5	7.6 ± 0.7	4.2 ± 0.5

[a]Amount of absorbed radiation (pmol photons $cell^{-1}$ d^{-1}).
[b]Cellular dry weight at the start of light period (pg $cell^{-1}$).
[c]Growth rate (d^{-1}).
[d]Growth efficiency was derived from (μ/Q_{phar}) [(nmol photons)$^{-1}$].
Data are given as mean values of three sampling days ± standard deviation.

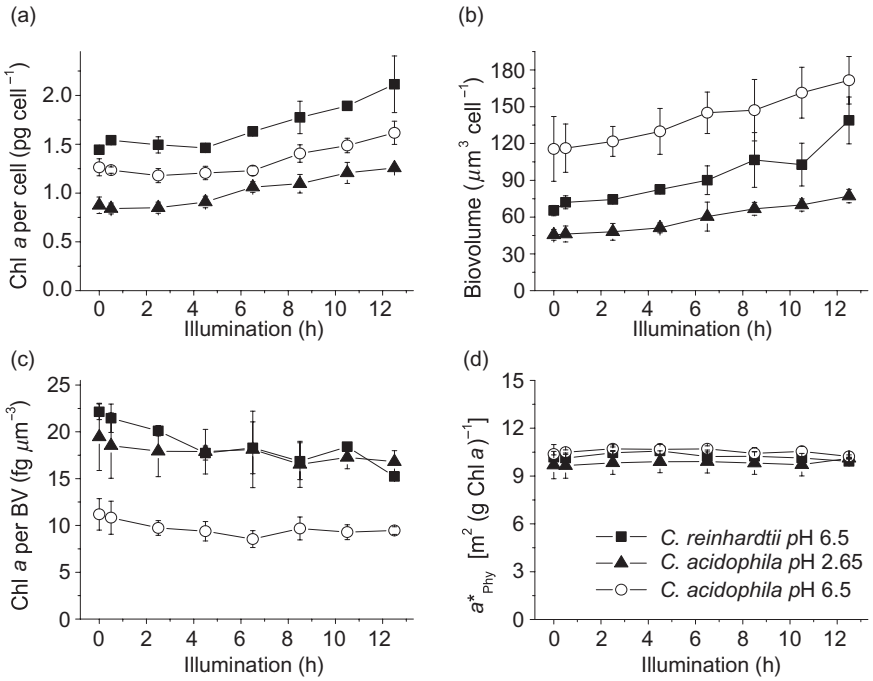

Figure 1. Variability of (a) Chl *a* per cell, (b) biovolume per cell, (c) Chl *a* per biovolume and (d) Chl *a*-specific *in vivo* absorption coefficient a^*_{phy} in *Chlamydomonas reinhardtii* (filled squares), *C. acidophila* (pH 2.6; filled triangles) and *C. acidophila* (pH 6.5, open circles) in the course of the light phase. Data are given as mean values of three sampling days ± standard deviation.

efficiency, with the result that the average Chl *a*-specific absorption efficiency did not show a dial variability and was similar among all three varieties (Table 1). Keeping in mind the different amounts of pigment per cell, *C. reinhardtii* absorbed approximately 60% more photons per cell and time compared with *C. acidophila* at pH 2.6, and 20% more than *C. acidophila* at pH 6.5 (Table 1).

Changes in photosynthetic efficiency

The number of photons needed to produce a new cell can be influenced either by the quantum efficiency of the photosynthetic primary reactions or by alternative electron pathways that guide the electrons liberated from PSII to acceptors other than carbon or nitrogen. The photosynthetic efficiency can be measured using pulse-modulated fluorescence, which allows an estimate of the energy used for photochemistry, the so-called qP, and the sum of all dissipating processes, 1-Φ_{PSII} (van Kooten & Snel 1990). (1-Φ_{PSII}) provides an estimate of the percentage of energy that is lost via non-photochemical dissipation. Figure 2 shows that this value was kept constant, between 35 and 37% of the absorbed quanta, under extreme acidity and in both *Chlamydomonas* species. As a consequence, the total electron flow from PSII (P_F) in all investigated *Chlamydomonas* species was determined only by the cellular absorption capacity. However, the amount of oxygen released per photon absorbed differed significantly between the three experimental varieties. In principle, if P_O equaled P_F, all electrons delivered from PSII would be used for the reduction of carbon or nitrogen. It must be emphasized that the medium used for the cultivation of algae contained ammonium as an N source; thus, there is no additional electron requirement for the incorporation of N in the biomass. On the other hand, if P_F is higher than P_O, a proportion of electrons of PSII is traced back to oxygen via different reactions, where oxygen functions as electron acceptor. This can be the Mehler reaction, photorespiration or light-increased mitorespiration. Another possibility for increasing the ratio P_F to P_O is to reduce the oxidized donor of PSII, not from the water splitting apparatus, but by cyclic flow around PSII (Prasil *et al.* 1996). Some of these processes can readjust the ATP/NADPH ratio and are needed, for instance, under carbon limiting conditions where a higher

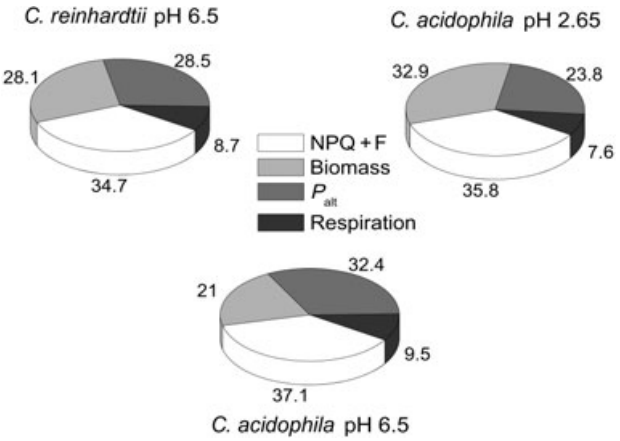

Figure 2. Photon usage in *Chlamydomonas reinhardtii*, *C. acidophila* (pH 2.6) and *C. acidophila* (pH 6.5) with respect to non-photochemical dissipation of absorbed light by heat and fluorescence (NPQ + F), alternative electron sinks (P_{alt}), respiration and biomass production. Values are given as percent of absorbed light (Q_{phar}) with the assumption that one molecule oxygen evolved/consumed equals eight photons absorbed and in consideration of the respiratory quotient (*RQ*).

Table 2. Gross photosynthesis rates in *Chlamydomonas reinhardtii* grown at pH 6.5 and in *C. acidophila* grown at pH 2.6 and 6.5

Parameter	*C. reinhardtii* pH 6.5	*C. acidophila* pH 2.6	*C. acidophila* pH 6.5
$\bar{P}_F$[a]	271 ± 14	263 ± 11	279 ± 9
$\bar{P}_O$[b]	150 ± 5	163 ± 9	127 ± 10
P_F[c]	6.0 ± 0.1	3.6 ± 0.3	4.8 ± 0.1
P_O[d]	3.3 ± 0.1	2.2 ± 0.2	2.3 ± 0.1
P_{alt}[e]	2.7 ± 0.2	1.4 ± 0.2	2.5 ± 0.1
$P_{alt}^{\%}$[f]	44 ± 2	38 ± 1	53 ± 1

[a]Averaged fluorescence-based photosynthesis rate [μmol O_2 (mg Chl*a*)$^{-1}$ h^{-1}].
[b]Averaged oxygen-based photosynthesis rate per light phase [μmol O_2 (mg Chl*a*)$^{-1}$ h^{-1}].
[c]Integrated fluorescence-based photosynthesis rate per light phase (pmol O_2 cell^{-1}).
[d]Integrated oxygen-based photosynthesis rate per light phase (pmol O_2 cell^{-1}).
[e]Alternative electrons are denoted as electrons that are not used in CO_2 fixation by the Calvin cycle and have been approximated by the difference ($P_F - P_O$) (pmol O_2 cell^{-1}).
[f]Alternative electrons per light phase given in relative amounts as percent of P_F.
Data are given as mean values of three sampling days ± standard deviation.

ATP/NADPH ratio is required for carbon concentrating processes. Here, we sum these electrons as 'alternative'. As outlined in Table 2, *C. acidophila* at pH 2.6 has a distinctly lower value for alternative electron cycling. In both *Chlamydomonas* strains grown at pH 6.5, alternative electron sinks consumed 50–55% of total number of electrons released at PSII, whereas *C. acidophila* at pH 2.6 can keep this process at a level of 39%. In relation to Q_{phar}, this means that in *C. reinhardtii* and *C. acidophila* (pH 6.5), 29 and 32% of the absorbed quanta, respectively, are directed into alternative electron sinks. In *C. acidophila* at pH 2.6, only 24% of the absorbed quanta can be found in alternative electron sinks (Fig. 2). It is important to note that this difference can be measured only if electron flow data obtained from fluorescence quenching analysis are compared with direct oxygen measurement, both related to absorbed photons.

Respiratory losses and macromolecular composition of the biomass

An energy balance from photons to carbon stored in the biomass must take into account the losses by respiration and the reduction of photosynthetically fixed carbon to synthesize the cellular macromolecules carbohydrates, proteins and lipids that account for approximately 95% of total dry weight (Zhu & Lee 1997; Kroon & Thoms 2006).

The total respiration per day was found to be 1.7 times higher in *C. acidophila* at pH 6.5 than in *C. reinhardtii* and *C. acidophila* at pH 2.6 (Table 3). However, taking into account the amount of cellular light absorption (see earlier discussion) and the respiratory quotient (Table 3), the respiratory losses of photosynthetically absorbed quanta were found to be comparable among the investigated *Chlamydomonas* strains (Fig. 2).

The macromolecular composition of the three species showed minor differences at the beginning of the light period. This becomes obvious from the C/N ratio, which was only slightly higher in *C. acidophila* compared with *C. reinhardtii* (Table 3). These data correlate with the macromolecular composition determined by means of FTIR spectroscopy. Here, a relatively higher content of carbohydrates and lipids at the expense of proteins was observed in *C. acidophila* compared with *C. reinhardtii* (Table 4). Thus, there are no differences in the degree of reduction of the biomass at the start of the light period. Nevertheless, during the light phase, the C/N ratio rose to a much higher ratio in *C. acidophila* under both pH conditions (Table 3), indicating pronounced changes in the macromolecular composition in this species. Figure 3 shows the daily increase in the cellular contents of newly synthesized carbohydrates, proteins and lipids in the comparison of *C. reinhardtii* and *C. acidophila* at pH 2.6 and 6.5. In *C. reinhardtii*, there was a proportional increase of all macromolecular components in the light period, whereas there was a slight decrease in all macromolecules during the dark period (Fig. 3a). Thus, there was only a slight increase in C/N during the light period. In general, the data indicate that the macromolecular composition in *C. reinhardtii* remained in a relatively balanced state. In contrast, a clear imbalance in the macromolecular composition between the light period and the subsequent dark period was visible in *C. acidophila* at pH 2.6 (Fig. 3b). During the first 4 h of the light period, the cells funnel their newly assimilated carbon mainly into carbohydrates and proteins but not into lipids. In comparison with *C. reinhardtii*, there was a stronger increase in carbohydrate content. In the remaining part of the light period, a slight increase in the synthesis of lipids was observed. However, the major proportion of lipid synthesis was found during the dark period. This led to a strong diurnal cycle in the C/N ratio in *C. acidophila* grown at pH 2.6 (Table 3). The general pattern of synthesis of macromolecules in *C. acidophila* pH 6.5 was comparable with *C. acidophila* grown at pH 2.6 (Fig. 3c). Moreover, the synthesis of a highly reduced macromolecular compound like lipids might be related to the increased respiration rates during the dark period as observed in *C. acidophila* at pH 2.6 and 6.5 (Table 3), which is also indicated by the concomitant decrease of newly synthesized carbohydrates (Fig. 3b,c).

DISCUSSION

Extremely acidic aquatic environments are expected to require specific cellular adaptations of photosynthetically active organisms. Thus, specific cell wall proteins are necessary when exposed to acidic conditions (Messerli *et al.* 2005). Because algal cells living at a low pH maintain an almost neutral cytosolic pH, a positive membrane potential (Gimmler *et al.* 1989), a decreased cytosolic membrane

Table 3. Mitochindrial respiration rates, respiratory quotient, daily carbon production and C/N ratios of the cells of *Chlamydomonas reinhardtii* grown at pH 6.5 and *C. acidophila* grown at pH 2.6 and 6.5

Parameter	*C. reinhardtii* pH 6.5	*C. acidophila* pH 2.6	*C. acidophila* pH 6.5
R_L[a]	1.01 ± 0.08	0.53 ± 0.14	0.98 ± 0.05
R_D[b]	0.23 ± 0.14	0.39 ± 0.10	0.53 ± 0.16
R[c]	1.25 ± 0.21	0.93 ± 0.19	1.50 ± 0.12
RQ	0.66 ± 0.08	0.49 ± 0.19	0.53 ± 0.17
B_C[d]	11.0 ± 0.7	8.5 ± 0.8	6.6 ± 1.0
C/N[e] (start of light period)	5.4 ± 0.05	5.6 ± 0.09	5.8 ± 0.07
C/N[e] (end of light period)	5.9 ± 0.05	6.9 ± 0.06	8.0 ± 0.61

[a]Integrated light-affected respiration rate (pmol O_2 cell^{-1} d^{-1}).
[b]Integrated dark respiration rate (pmol O_2 cell^{-1} d^{-1}).
[c]Integrated total respiration (pmol O_2 cell^{-1} d^{-1}).
[d]Daily carbon production (pg C cell^{-1} d^{-1}).
[e]Molar ratio carbon to nitrogen.
Data are given as mean values of three sampling days ± standard deviation.

permeability for protons (Gross 2000) and specific ATP-driven ion pumps (Sekler, Gläser & Pick 1991) are inevitable. In particular, the increased proton-pumping activity is assumed to be related to the elevated metabolic costs. These increased maintenance energy requirements have been illustrated in part by higher respiration rates and lower growth rates at non-saturating light intensities of *C. acidophila* grown at pH 2.6 compared with *C. reinhardtii* at pH 7 (Gerloff-Elias, Spijkerman & Pröschold 2005; Messerli *et al.* 2005). However, there is no evidence for an increased ATP requirement in *C. acidophila* grown at pH 2 (Messerli *et al.* 2005). Finally, it is not clear why the respiration rates in *C. acidophila* at low pH are increased, or if they are directly responsible for the lower growth rates.

In this study, we present a comparison of the energy balance of *C. reinhardtii* (pH 6.5) and of *C. acidophila* grown at pH 2.6 and 6.5 under turbidostat conditions with constant growth rates. Under these conditions, an energy balance allows the evaluation of the efficiency of metabolic processes on different levels, including the primary photosynthetic reaction, the activity of alternative electron sinks, respiration, and the electron requirement for the major macromolecular compounds.

The first surprising result of the present study was the observation that, despite the lower growth rates, the quantum efficiency of growth in *C. acidophila* at pH 2.6 was higher compared with *C. reinhardtii* at pH 6.5. Whereas the quantum efficiency of the primary photosynthetic reaction at PSII was comparable in all investigated *Chlamydomonas* species, another unexpected result was found in the activity of alternative electron pathways. It has been suggested by several authors that 'alternative' electron cycling is an efficient strategy to produce more ATP needed for stress compensation. Our data show exactly the contrast: alternative electron cycling was lowest in *C. acidophila* at pH 2.6 compared with *C. reinhardtii* and to *C. acidophila* grown at pH 6.5. Thus, if there is a need for additional ATP under low pH, it is not provided by reactions in the chloroplast, but might be supplied by mitochondrial ATP production.

Table 4. Macromolecular composition of the cells of *Chlamydomonas reinhardtii* grown at pH 6.5 and *C. acidophila* grown at pH 2.6 and 6.5 at the start of the light phase

Parameter	*C. reinhardtii* pH 6.5	*C. acidophila* pH 2.6	*C. acidophila* pH 6.5
Carbohydrates	9.1 ± 0.2	11.9 ± 0.3	14.8 ± 1.9
Proteins	69.5 ± 1.0	62.4 ± 1.5	63.1 ± 2.8
Lipids	17.3 ± 1.1	24 ± 1.4	20.6 ± 5.4

Data are given as mean values of three sampling days ± standard deviation (% weight per cellular dry weight).

The macromolecular composition of a cell determines the electron requirement per carbon fixed in the biomass, for example, the energy requirement is drastically reduced under nitrogen-limited conditions because of the shift in the biomass composition from highly reduced proteins to less reduced carbohydrates (Jakob *et al.* 2007). Interestingly, the reduction degree of the biomass is unchanged, on average, between neutral and acidic conditions. The macromolecular composition of the biomass was almost identical at the beginning of the light period among the different *Chlamydomonas* species, but changed during the light phase between *C. reinhardtii* and *C. acidophila*. Whereas in *C. reinhardtii* a proportional increase in all macromolecules was observed, under acidophilic conditions, the carbon was preferentially incorporated into carbohydrates in the light phase, but in the following dark period the biomass was converted into higher reduced lipids. We propose that this metabolic reorganization is related to the increased dark respiration in *C. acidophila*.

Taken together, the data clearly show that the energy usage is more efficient in *C. acidophila* at pH 2.6 compared with the wild strain. Thus, the major reason for the lower growth rates of *C. acidophila* at pH 2.6 is the reduced light capture capacity. The highest quantum efficiency of growth in combination with the lower growth rates in *C. acidophila* at pH 2.6 might appear somewhat contradictory; however, we believe that this effect is caused by carbon limitation. Under acidic conditions the carbon delivery is limited to

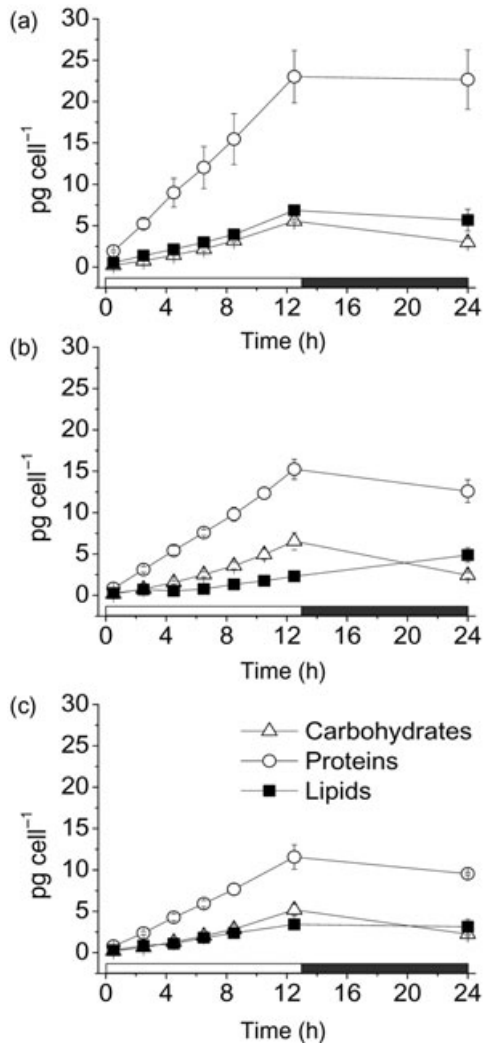

Figure 3. Daily increase in the cellular contents of newly synthesized carbohydrates (open triangles), proteins (open circles) and lipids (filled squares) in the comparison of *Chlamydomonas reinhardtii* (a) and *C. acidophila* at pH 2.6 (b) and pH 6.5 (c). The white and black bars on the *x*-axis indicate the light and dark phase, respectively. Data are given as mean values of three sampling days ± standard deviation.

free CO_2 (Stumm & Morgan 1970). Although *C. acidophila* is well adapted to carbon-limited conditions (Tittel *et al.* 2005), it is known that the extent of carbon limitation is indicated by the ratio Chl *a*/carbon (e.g. Geider 1987). In the present study, a Chl *a*/C ratio of 0.067 was found for *C. reinhardtii*, compared with a value of 0.035 for *C. acidophila* grown at pH 2.6 (data not shown). Tittel *et al.* (2005) reported a Chl *a*/C ratio of 0.039 for *C. acidophila* grown under high light and low CO_2 and 0.071 at high CO_2 conditions. This indicates carbon limiting conditions for *C. acidophila* at pH 2.6, but not for *C. reinhardtii*.

The energy balance of both species of *Chlamydomonas* under different growth conditions also revealed that the growth of *C. acidophila* at pH 6.5 was the most stressful condition. This is indicated by the lowest growth rates, the highest activity of alternative electron consuming reactions, and the highest respiration rates in comparison with *C. reinhardtii* and *C. acidophila* at pH 2.6. These drastically increased metabolic costs, yielded in a 46 and 25% lower quantum efficiency of growth in *C. acidophila* at pH 6.5 in comparison with *C. acidophila* at pH 2.6 and *C. reinhardtii*, respectively. Messerli *et al.* (2005) suggested that the reduced growth of acidophilic species at higher pH is related to the working pH range of cell wall enzymes.

The present study shows that environmental conditions can force algal cells to vary not only the efficiency of the photosynthetic apparatus and the cellular maintenance costs, but also to reorganize metabolic pathways. This complexity of regulation is not detectable by fluorescence or gas exchange measurements alone; even the partial analysis of the regulation of the key enzymes does not reveal the changes in fluxes that finally define the growth rate. The present study shows that a combination of bio-optical modelling and the measurement of changes in the macromolecular composition of cells is a powerful tool to monitor metabolic fluctuations. Recently, it was shown that FTIR spectroscopy allows measurement of the overall macromolecular composition with a time resolution of 30 min, which helps to identify key events in regulation (Stehfest 2006). In conclusion, bio-optical modelling, together with macromolecular FTIR-based fingerprinting, is an appropriate tool to monitor oscillations in the time scale of diurnal rhythms or within hours in response to environmental disturbances. This technique may therefore be an indispensable approach for future optimization of algal photobioreactors using transgenic *Chlamydomonas* strains.

ACKNOWLEDGMENT

Financial support of the Deutsche Forschungsgemeinschaft (grant number Wi 764/12-1) is greatly acknowledged.

REFERENCES

Asada K. (2000) The water–water cycle as alternative photon and electron sinks. *Philosophical Transactions of the Royal Society of London. Series B, Biological Sciences* **355,** 1419–1431.

Davies J.P. & Grossman A.R. (1998) The use of *Chlamydomonas* (Chlorophyta: Volvocales) as a model algal system for genome studies and the elucidation of photosynthetic processes. *Journal of Phycology* **34,** 907–917.

Dent R.M., Han M. & Niyogi K.K. (2001) Functional genomics of plant photosynthesis in the fast lane using *Chlamydomonas reinhardtii*. *Trends in Plant Science* **6,** 364–371.

Falkowski P.G. & Raven J.A. (1997) *Aquatic Photosynthesis*. Blackwell Science, Malden, MA, USA.

Finazzi G. & Forti G. (2004) Metabolic flexibility of the green alga *Chlamydomonas reinhardtii* as revealed by the link between state transitions and cyclic electron flow. *Photosynthesis Research* **82,** 327–338.

Geel C., Versluis W. & Snel J.F.H. (1997) Estimation of oxygen evolution by marine phytoplankton from measurement of the efficiency of Photosystem II electron flow. *Photosynthesis Research* **51,** 61–70.

Geider R. (1987) Light and temperature dependence of the carbon

to chlorophyll a ratio in microalgae and cyanobacteria: Implications for physiology and growth of phytoplankton. *New Phytologist* **106,** 1–34.

Genty B., Briantais J.-M. & Baker N.R. (1989) The relationship between the quantum yield of photosynthetic electron transport and quenching of chlorophyll fluorescence. *Biochimica et Biophysica Acta* **990,** 87–92.

Gerloff-Elias A., Spijkerman E. & Pröschold T. (2005) Effect of external pH on the growth, photosynthesis and photosynthetic electron transport of *Chlamydomonas acidophila* Negoro, isolated from an extremely acidic lake (pH 2.6). *Plant, Cell & Environment* **28,** 1218–1229.

Gilbert M., Domin A., Becker A. & Wilhelm C. (2000) Estimation of primary productivity by chlorophyll a *in vivo* fluorescence in freshwater phytoplankton. *Photosynthetica* **38,** 111–126.

Gimmler H., Weis U., Weiss C., Kugel H. & Treffny B. (1989) *Dunaliella acidophila* (Kalina) Masyuk – an alga with a positive membrane potential. *New Phytologist* **113,** 175–184.

Gross W. (2000) Ecophysiology of algae living in highly acidic environments. *Hydrobiologia* **433,** 31–37.

Grossman A.R. & Rokhsar D.S. (2007) Alga genome data may help biodiesel production. *Industrial Bioprocessing* **29,** 4–5.

Grube M., Zagreba E., Gromozova E. & Fomina M. (1999) Comparative investigation of the macromolecular composition of mycelia forms *Thielavia terrestris* by infrared spectroscopy. *Vibrational Spectroscopy* **19,** 301–306.

Jakob T., Wagner H., Stehfest K. & Wilhelm C. (2007) A complete energy balance from photons to new biomass reveals a light- and nutrient-dependent variability in the metabolic costs of carbon assimilation. *Journal of Experimental Botany* **58,** 2101–2112.

van Kooten O. & Snel J.F.H. (1990) The use of chlorophyll fluorescence nomenclature in plant stress physiology. *Photosynthesis Research* **25,** 147–150.

Kroon B.M.A. & Thoms S. (2006) From electron to biomass:a mechanistic model to describe phytoplankton photosynthesis and steady state growth rates. *Journal of Phycology* **42,** 593–609.

Melis A., Seibert M. & Ghirardi M.L. (2007) Hydrogen fuel production by transgenic microalgae. *Advances in Experimental Medicine and Biology* **616,** 110–121.

Messerli M.A., Amaral-Zettler L.A., Zettler E., Jung S.K., Smith P.J.S. & Sogin M.L. (2005) Life at acidic pH imposes an increased energetic cost for a eukaryotic acidophile. *Journal of Experimental Biology* **208,** 2569–2579.

Mittag M. & Wagner V. (2003) The circadian clock of the unicellular eukaryotic model organism *Chlamydomonas reinhardtii*. *Biological Chemistry* **384,** 689–695.

Mussgnug J.H., Thomas-Hall S., Rupprecht J., Foo A., Klassen V., McDowall A., Schenk P.M., Kruse O. & Hankamer B. (2007) Engineering photosynthetic light capture: impacts on improved solar energy to biomass conversion. *Plant Biotechnology Journal* **5,** 802–814.

Nichols H.W. (1973) Growth media-freshwater. In *Handbook of Phycological Methods: Culture Methods an Growth Measurements* (ed. J.R. Stein), pp. 7–24. Cambridge University Press, Cambridge, UK.

Prasil O., Kolber Z., Berry J.A. & Falkowski P.G. (1996) Cyclic electron flow around Photosystem II in vivo. *Photosynthesis Research* **48,** 395–410.

Prasil O., Suggett D.J., Cullen J.J., Babin M. & Govindjee (2008) Aquafluo 2007: chlorophyll fluorescence in aquatic sciences, an international conference held in Nové Hrady. *Photosynthesis Research* **95,** 111–115.

Purton S. (2007) Tools and techniques for chloroplast transformation of *Chlamydomonas*. *Advances in Experimental Medicine and Biology* **616,** 34–45.

Rochaix J.D. (2004) Genetics of the biogenesis and dynamics of the photosynthetic machinery in eukaryotes. *The Plant Cell* **16,** 1650–1660.

Schmidt M., Geßner G., Luff M., *et al.* (2006) Proteomic analysis of the eyespot of *Chlamydomonas reinhardtii* provides novel insights into its components and tactic movements. *The Plant Cell* **18,** 1908–1930.

Sekler I., Gläser H.U. & Pick U. (1991) Characterization of a plasma membrane H^+-ATPase from the extremely acidophilic alga *Dunaliella acidophila*. *Journal of Membrane Biology* **121,** 51–57.

Stauber E.J. & Hippler M. (2004) *Chlamydomonas reinhardtii* proteomics. *Plant Physiology and Biochemistry* **42,** 989–1001.

Stehfest K. (2006). *Die FT-IR-Spektroskopie in der Pflanzenphysiologie – Anwendungsmöglichkeiten für die Zellinhaltsstoffanalytik*. PhD thesis, University Leipzig, Leipzig, Germany.

Stehfest K., Toepel J. & Wilhelm C. (2005) The application of micro-FTIR spectroscopy to analyze nutrient stress-related changes in biomass composition of phytoplankton algae. *Plant Physiology and Biochemistry* **43,** 717–726.

Stumm W. & Morgan J.J. (1970) *Aquatic Chemistry: Chemical Equilibria and Rates in Natural Waters*. Wiley Interscience, New York, NY, USA.

Suggett D.J., Oxborough K., Baker N.R., Macintyre H.L., Kana T.M. & Geider R.J. (2003) Fast repetition rate and pulse amplitude modulation chlorophyll a fluorescence measurements for assessment of photosynthetic electron transport in marine phytoplankton. *European Journal of Phycology* **38,** 371–384.

Suggett D.J., Maberly S.C. & Geider R.J. (2006) Gross photosynthesis and lake community metabolism during the spring phytoplankton bloom. *Limnology and Oceanography* **51,** 2064–2076.

Tittel J., Bissinger V., Gaedke U. & Kamjunke N. (2005) Inorganic carbon limitation and mixotrophic growth in *Chlamydomonas* from an acidic mining lake. *Protist* **156,** 63–75.

Wagner H., Jakob T. & Wilhelm C. (2006) Balancing the energy flow from captured light to biomass under fluctuating light conditions. *New Phytologist* **169,** 95–108.

Wilhelm C. & Wild A. (1984) The variability of the photosynthetic unit in Chlorella II. The effect of light intensity and cell development on photosynthesis, P-700 and cytochrome f in homocontinuous and synchronous cultures of *Chlorella*. *Journal of Plant Physiology* **115,** 124–135.

Zhu C. & Lee Y. (1997) Determination of biomass dry weight of marine microalgae. *Journal of Applied Phycology* **9,** 189–194.

Ziegler R. & Egle K. (1965) Zur quantitativen Analyse der Chloroplastenpigmente. I. Kritische Überprüfung der spektralphotometrischen. Chlorophyllbestimmung. *Beiträge zur Biologie der Pflanze* **41,** 11–37.

Received 8 September 2008; accepted for publication 27 October 2008

